Effect of hydrogen bonds on polarizability of a water molecule in $(H_2O)_N$ (N = 6, 10, 20) isomers†

Fang Yang,[a] **Xin Wang,**[a] **Mingli Yang,***[a] **Alisa Krishtal,**[b] **Christian van Alsenoy,**[b] **Patrice Delarue**[c] **and Patrick Senet***[c]

Polarizabilities of the low-lying isomers of $(H_2O)_N$ (N = 6, 10, 20) clusters were computed by using Density Functional Theory. The global polarizabilities of the water isomers were found to depend mainly on the total number of water molecules rather than their cluster structures. We show that this result hides in fact a strong heterogeneity of the molecular polarizability within the different isomers. The global polarizability of a cluster was divided into a sum of molecular contributions by using the Hirshfeld partitioning scheme. We reveal that the value of the local polarizability of a molecule in the cluster is correlated with the number and type of the hydrogen bonds (HB) the molecule forms. Consequently, the molecules located in the interior of the cluster, which usually form more HBs, have smaller molecular polarizabilities than the molecules at the surface, which form less HBs. The contribution of intermolecular interaction to the global polarizability was analyzed by decomposing the cluster polarizability into intra- and inter-molecular contributions. The former measures the polarization within the molecular basin against the external electric field, while the latter is described as the sum of polarizability caused by charge flow through the HBs. These two contributions vary with the cluster size: the intermolecular contribution decreases with the cluster size on the contrary of the intramolecular contribution which increases.

1. Introduction

Water clusters (W_N, where N is the aggregation number) are intermediate systems between gas phase and condensed phases and offer the opportunity to understand how the properties of bulk water emerge and how the properties of water may change with size. There have been many experimental and theoretical studies of water clusters focusing on the determination of the most stable structures, the corresponding stabilization energies, and of the harmonic vibrational frequencies *etc*.[1–36]

The structure of water clusters depend on their size. The most stable structure of W_2 is linearly hydrogen bonded, while W_3–W_5 are monocyclic rings.[2,6] For clusters larger than W_5, there remains some uncertainty on the most stable structures. For example, W_6 has several stable isomers such as the hexamer cage, prism, ring, book, bag, *etc*., which are nearly isoenergetic. Recent theory and experiment have suggested the cage to be the most stable form.[4,6,8,32] As the aggregation number increases, the number of local minima on the potential energy surface grows exponentially and the number of stable and metastable structures is expected to be large.

The size dependence of the dielectric properties of water clusters have attracted recent attention because of their importance in understanding the intermolecular interaction between water molecules.[37–49] In contrast to the intensive studies of the dipole moment of water,[6,42,37–39,50–52] only few works concerned the study of the water polarizability,[43,44,49,53–58] which is an essential ingredient for describing intermolecular interactions.

The size-dependence of polarizability of water clusters was firstly studied by Rodriguez *et al.*[57] with density functional theory (DFT) using generalized gradient approximation (GGA) functionals for W_2 to W_8 clusters. In a systematic investigation of the polarizability of the most stable isomers of W_2 to W_{20}, Ghanty and Gosh[58] found that the polarizability of a water cluster, computed at Hartree–Fock (HF) and for W_2 to W_{10} at DFT level (using the hybrid B3LYP functional) and at Møller–Plesset second order approximation (MP2) levels, increases linearly with the number of molecules in the cluster. Their results, suggested a simple additive model to estimate the polarizabilities of large water clusters. Very recently, Hammond *et al.*[49] computed the polarizabilities of W_2 to W_{12} at the coupled-cluster level of theory (CCSD) and used these data to benchmark the density functionals and basis sets for the polarizability calculations. In our previous studies,[43,44] the size dependence of the polarizability, as well as its correlation with HBs, has been addressed for the most-stable water clusters with DFT method. We will prove below that the linear size-dependence of polarizability for the most

[a] Institute for Nanobiomedical Technology and Membrane Biology, West-China Hospital, Sichuan University, Chengdu 610041, China. E-mail: myang@scu.edu.cn
[b] Structural Chemistry Group, Department of Chemistry, University of Antwerp, Universiteitsplein 1, B-2610 Antwerp, Belgium
[c] Institut Carnot de Bourgogne, UMR 5209 CNRS-Université de Bourgogne, 9 Av. A. Savary, BP 47870, F-21078 Dijon Cedex, France. E-mail: patrick.senet@u-bourgogne.fr
† Electronic supplementary information (ESI) available: Table 1S: Intramolecular harmonic vibrational frequency ranges of water clusters calculated with B3LYP/6-311G(d,p). See DOI: 10.1039/c001007c

This journal is © the Owner Societies 2010

Phys. Chem. Chem. Phys., 2010, **12**, 9239–9248 | 9239

stable structures of W_2 to W_{20} predicted from the previous computational studies[43,44,58] can be applied to water isomers that possess different structures from the most stable ones.

The polarizability of a water molecule within a condensed phase is expected to be different from its value in the gas phase because of inter-molecular interactions. However, little is known about the variation of polarizability of a molecule in weakly bonded systems such as water clusters, in which the molecules are linked with each other through hydrogen bonds. Some authors have argued theoretically that the molecular polarizability of water decreases in condensed phase.[39,59,60] Moreover, in het Panhuis et al.[61] have pointed out that the two molecules in the water dimer have different molecular polarizabilities. On one hand, studies have shown that the intermolecular interaction in water clusters influence considerably the polarizability of a water molecule within the cluster.[61] On the other hand, the simple additive rule[58] to estimate the polarizabilities of large water clusters implies little effect of intermolecular interaction on the polarizabilities of clusters. In order to understand the origin of the linear dependence of the cluster polarizability with the cluster size, we carried out a computational study of both the cluster and molecular polarizabilities of the isomers of W_6, W_{10} and W_{20}. The variation of the polarizability of a cluster with its structure, as well as the polarizability of a molecule with its location and hydrogen bonding, were investigated in detail.

In this study, the polarization of individual molecules in water clusters is investigated with *ab initio* calculations, combined with the Hirshfeld partitioning scheme.[62,63] Our calculations show that the molecules within a cluster contribute differently to the cluster polarization depending on the HBs they form with the surrounding molecules. Despite this fact, the additive rule to estimate the cluster polarizability holds in general for the water isomers. In addition, by decomposing the cluster polarizability into intra- and inter-molecular parts, we found a direct correlation between the polarizability of a cluster and the intermolecular polarization through HBs. Our results reveal the important role of HBs in the polarization of water clusters.

2. Method

All the ground-state structures shown in Fig. 1 were optimized at the B3LYP/6-311G(d,p) level starting with the HF/6-31G(d,p) geometries[5] taken from the Cambridge Cluster Database (CCD).[64] The frequency calculations were carried out at the same level to determine the harmonic frequencies, as well as to ensure that the obtained structures are the local minima on the corresponding energy potential surfaces. It is known that the addition of polarization and diffuse functions to the basis set is essential to generate reliable results of polarizability.[65–67] The basis sets of 6-311++G(d,p) and aug-cc-PVDZ, which contain augmented diffuse functions, are thus employed in the polarizability calculations. Hammond et al.[49] found that the combination of PBE0 functional and the aug-cc-pVDZ basis set produces overall accurate polarizabilities at a moderate computational cost. They also found the differences between aug-cc-pVDZ and aug-cc-pVTZ results decrease smoothly with increasing size, about 0.6% for W_6 and about 0.1%

for W_{10}. The aug-cc-pVDZ basis set was considered as a reasonable option in calculating the polarizabilities for large water clusters. Our previous studies[43,44] have illustrated that the polarizabilities computed using DFT are quite similar to the ones obtained using MP2 for water clusters of $N \leq 15$. In the present work, the polarizabilities are computed with the B3LYP[68,69] and PW91[70] functionals and MP2 for the isomers of W_6, W_{10} and W_{20}.

In the finite-field (FF) approach,[71,72] the polarizability can be formulated as the numerical difference of the total energy or dipole moment of the system with respect to the applied field. By carefully selecting the strength of the applied electric field, one may obtain a reliable value of the polarizability excluding contamination from higher-order perturbation terms.[65,67] The applied field strength in the FF calculation is set to 0.001 au and the SCF convergence criteria are tightened to 10^{-8} au in density. Both FF approaches, energy-based and dipole moment-based, can be used to calculate the cluster polarizabilities. The dipole moment-based is used in this study. The dipole moment of the water molecule in the cluster, $\boldsymbol{\mu}$, is given by[73]

$$\boldsymbol{\mu} \equiv \sum_{k=1}^{3} [\boldsymbol{p}_k + q_k \boldsymbol{r}_k] \qquad (1)$$

where k denotes the kth atom in the molecule. q_k and $\boldsymbol{p}_k$ are respectively the net atomic charge and atomic dipole of the kth atom, obtained with the Hirshfeld scheme.[62,63] $\boldsymbol{r}_k$ is the position of the kth atom (nucleus). It should be noted that the individual molecules in a water cluster are generally charged due to the intermolecular charge transfer through the hydrogen bonds.[74,75] As a result, the molecular dipole moment, $\boldsymbol{\mu}$, obtained from eqn (1) depends on the location of the origin of the Cartesian axes chosen in the calculation, so is the molecular polarizability computed by using the FF approach. To be able to compare the polarizabilities of the different molecules within a cluster, one must define the dipole of a molecule relative to its position in the cluster. We choose this position to be the geometrical center of each molecule, which is defined as $\boldsymbol{R}_L \equiv \frac{1}{3}\sum_{k=1}^{3} \boldsymbol{r}_k$. The dipole moment of molecule L is then written as

$$\boldsymbol{\mu}_L = \boldsymbol{\mu}_L^{\text{c}} + Q_L \boldsymbol{R}_L \qquad (2)$$

where Q is the sum of the atomic charges of the three atoms of the molecule and $\boldsymbol{\mu}^{\text{c}}$ is the so-called corrected dipole moment of the molecule

$$\boldsymbol{\mu}_L^{\text{c}} \equiv \sum_{k=1}^{3} [\boldsymbol{p}_k + q_k(\boldsymbol{r}_k - \boldsymbol{R}_L)]. \qquad (3)$$

The corrected dipole $\boldsymbol{\mu}^{\text{c}}$ does not depend on the location of the origin of the Cartesian axes. This quantity reflects the intra-molecular polarization of a water molecule in a cluster.

The total electric field felt by a molecule within a cluster is the superposition of the applied field and the field induced by surrounding molecules

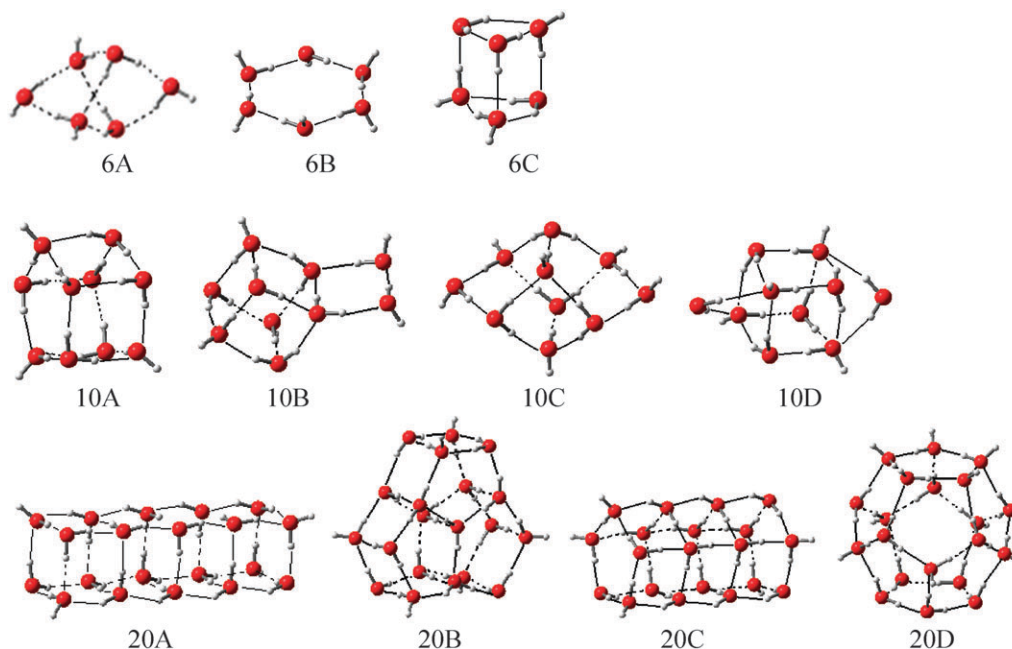$$\boldsymbol{E} = \boldsymbol{E}_{\text{appl}} + \boldsymbol{F}_{\text{ind}} \qquad (4)$$

Fig. 1 Structures of W_6, W_{10} and W_{20} isomers.

In point dipole models, the induced field can be approximated by[73]

$$F_{ind} = \sum_{L' \neq L} \frac{3(\Delta\mu_{L'} \cdot R_{L'L})R_{L'L} - R_{L'L}^2 \Delta\mu_{L'}}{R_{L'L}^5}, \quad (5)$$

where L' runs over all the molecules but L in the cluster and $R_{L'L} = R_{L'} - R_L$.

The polarizability tensor of a molecule in a cluster, α, can be defined by assuming a linear response as follows

$$\Delta\mu_L^c = \mu_L^c(E) - \mu_L^c(0) = \overset{\leftrightarrow}{\alpha}(F_{ext} + \Delta F_{ind}). \quad (6)$$

In this study we compare mean polarizabilities, which are computed by $\langle\alpha\rangle = (\alpha_{xx} + \alpha_{yy} + \alpha_{zz})/3$, among the water clusters and among the molecules in the clusters. The second term on the rhs of eqn (2) measures the charge-transfer contribution to the dipole moment. It is origin-dependent for the charged molecules. We will discuss the polarizabilities derived from the charge-transfer term in next section. All the calculations are performed with the Gaussian03 program[76] and the BRABO package.[77]

3. Results and discussion

3.1 Geometry and vibrational frequencies

The geometries and binding energies of the isomers have already been discussed by Maheshwary et al.[17] at HF and DFT levels for W_6 and W_{10} and at HF level for W_{20}. We present briefly in Table 1 some geometric parameters optimized at B3LYP/6-311G(d,p) level for the clusters shown in Fig. 1, as well as the relative energy with and without zero-point vibrational energy (ZPE) and basis set superposition error (BSSE) corrections. Here we follow Maheshwary's[17] notations: the hydrogen involved in a hydrogen bond is referred to as H_b and the one not involved as H_f. The mean

lengths of $O–H_b$ are different in the different isomers and obviously longer than the distance $O–H_f$, which is almost the same for all the water molecules. The isomers 6C, 10D and 20A form the largest number of HBs but have the longest average HB lengths, while the clusters 6B, 10C and 20D form the least number of HBs but have the shortest average HB lengths. The clusters 6C, 10A and 20A are most stable among the corresponding isomers, but the energy differences between 6A and 6C, 10A and 10B, 20A and 20C are rather small. The ZPE correction does not change the order in the energy, but 6B, 10A and 20C become the most stable when both ZPE and BSSE are included. 6A was predicted to be the most stable structure when the ZPE is included in some other calculations.[8,11] The performance of DFT in determining the energy minima for weakly bonded systems is still an open question.[13,28,32,78,79] It is not the purpose of this study to assess various density functionals in predicting the energy orders of water clusters. Instead, we focus on the general trend of the cluster and molecular polarizability variations with the structures. Our previous studies have demonstrated that DFT and MP2 calculations predict the same trends and similar values for the polarizabilities of water clusters.[43,44]

The frequency calculations give real frequencies for all the clusters, confirming that the optimized structures are local minima on the corresponding PES. The computed intra-molecular harmonic vibrational frequencies are given in ESI†. Our calculations are in agreement with other studies for the hexamers.[2,8,17] Different levels of theory predict the frequencies slightly different in magnitude, but reveal the fact that the intermolecular interactions in the water clusters have considerable influence on the vibrational frequencies. Using a combined double-harmonic approximation and finite-field approach, Pederson et al.[80] have found that the vibrational polarizabilities of W_2, W_3 and W_5 are larger than their electronic counterparts.

Table 1 Relative energy and averaged geometric parameters of water clusters[a]

W_N isomer	n_{HB}[b]	E_{rel}[c]	$E_{rel,ZPE}$[d]	$E_{rel,ZPE+BSSE}$[e]	$r_{O\cdots O}$	r_{O-Hf}[f]	r_{O-Hb}[f]	$r_{O\cdots H}$[g]
6A	8	0.0024 0.0015[h]	0.0019	0.0053	2.769	0.962	0.982	1.829
6B	6	0.0102 0.0000[h]	0.0069	0.0000	2.684	0.961	0.988	1.698
6C	9	0.0000 0.0004[h]	0.0000	0.0056	2.783	0.961	0.979	1.885
10A	15	0.0000 0.0000[h]	0.0000	0.0000	2.749	0.961	0.984	1.786
10B	15	0.0032 0.0047[h]	0.0034	0.0034	2.752	0.962	0.983	1.799
10C	14	0.0070 0.0034[h]	0.0055	0.0020	2.734	0.961	0.986	1.761
10D	16	0.0333 0.0275[h]	0.0277	0.0253	2.859	0.963	0.982	1.925
20A	36	0.0000	0.0000	0.0012	2.768	0.962	0.981	1.840
20B	34	0.0104	0.0074	0.0011	2.762	0.962	0.982	1.813
20C	35	0.0033	0.0018	0.0000	2.761	0.962	0.982	1.823
20D	30	0.0687	0.0598	0.0306	2.769	0.964	0.985	1.789

[a] Energy is in hartrees and the distances in Å. Geometry optimization was carried out with B3LYP/6-311(d,p). [b] Number of hydrogen bonds. [c] Relative energy. [d] Relative energy with ZPE correction. [e] Relative energy with ZPE and BSSE corrections. [f] See text for the notations. [g] Bond lengths of hydrogen bond. [h] Relative energy calculated with MP2/6-311++G(d,p).

In this study we restrict our study within the electronic polarizabilities of the W_6, W_{10} and W_{20} isomers.

3.2 Cluster polarizability

Table 2 lists the calculated dipole moments and polarizabilities of the W_6, W_{10} and W_{20} isomers, as well as a comparison with other computations. The dipole moments computed using the B3LYP and PW91 functionals give values which are very close to those obtained with MP2, while the basis set 6-311++G(d,p) tends to give larger values than the aug-cc-pVDZ basis set. The values of the cluster polarizabilities computed with aug-cc-pVDZ are larger than those obtained with 6-311++G(d,p) by around 10% but the variation of the cluster polarizability with its size is similar in both cases. The errors with respect to CCSD/aug-cc-PVDZ results[49] for W_6 and W_{10} are less than 1%. We will focus our discussion now on the aug-cc-pVDZ results.

The polarizabilities calculated using the PW91 functional are larger than those computed using the hybrid B3LYP functional and MP2 for all the isomers. However, all the three approaches give the same ordering of polarizabilities: 6B > 6A > 6C, 10C > 10B > 10A > 10D and 20D > 20B > 20A > 20C. B3LYP and MP2 produce very close results with deviations of less than 3% for W_6 and W_{10}.

The isomers 6A, 6B and 6C have very similar polarizabilities with a relative standard deviation of 1.50%. This is also true for W_{10} and W_{20} for which the relative standard deviations between the different isomers are only 0.81% and 0.67%, respectively. Such very small differences between the polarizabilities of the isomers indicate that the polarizabilities of water clusters are mainly dependent on their aggregation number rather than their geometries. These isomers are quite different in structure, as seen in Fig. 1, but possess almost the same polarizabilities. One may conclude that the simple additive model[58] deduced from the calculations for the most

stable structures of water clusters can be expanded to the isomers studied. All the isomers studied here are among the most stable conformations predicted by theoretical calculations.[17] Combining Table 1 and 2, one cannot find a direct correlation between the polarizability and stability. For example, both 10D and 20D have the highest energy among the isomers, but 10D has the smallest polarizability, whereas 20D has the polarizability larger than 20A and 20C.

The study of the water isomers, which have the same number of water molecules, provides a good means to examine the correlation between the number of HBs and the cluster polarizability. A larger correlation coefficient was obtained by Ghanty and Ghosh[58] when they used the number of HBs to replace the cluster size into the fitted linear relation between cluster polarizability and the cluster size. The present calculations show also some correlation between the polarizability of a cluster and its number of HBs. The structures 6C and 10D have 9 and 16 HBs, respectively and have the smallest polarizabilities, while 6B, 10C, 20D have 6, 14, 30 HBs, respectively and have the largest polarizabilities among the corresponding isomers. However, one should also notice that such correlation is not monotonic. 20A has one more HB than 20C, but its polarizability is 0.03 larger than that of 20C. It is clear that the number of HB is relevant to the cluster polarizability but the correlation is not explicit.

The average polarizability per molecule, defined as the quotient of the cluster polarizability divided by the aggregation number, does not change very much with the cluster size. Going from 6A to 20A leads to a decrease of 0.02 au at B3LYP level and 0.07 au at MP2 level, demonstrating a decreasing tendency when the cluster grows.

3.3 Molecular polarizability

A typical structural feature of water in condensed phase is a HB network in which each molecule donates its two protons

9242 | *Phys. Chem. Chem. Phys.*, 2010, **12**, 9239–9248

This journal is © the Owner Societies 2010

Table 2 Calculated dipole moments (μ) and cluster polarizabilities (α) of the W_6, W_{10} and W_{20} isomers[a]

	μ			α			α/N		
	B3LYP	PW91	MP2	B3LYP	PW91	MP2	B3LYP	PW91	MP2
				6-311++G(d,p)					
6A	0.870	0.860	0.861	53.12	57.05	50.94	8.85	9.51	8.49
	0.797[b]		0.820[c]	58.01[d]	42.49[e]				
					52.90[f]				
6B	0.000	0.000	0.000	53.31	57.01	51.21	8.88	9.50	8.53
	0.000[b]		0.000[c]		51.94[f]				
6C	1.111	1.094	1.101	53.04	57.02	50.82	8.84	9.50	8.47
	1.029[b]		1.067[c]		52.86[f]				
10A	1.058	1.046	1.047	90.01	96.52	86.60	9.00	9.65	8.66
				97.17[d]	72.15[e]				
10B	0.939	0.925	0.926	89.79	96.36	86.27	8.98	9.64	8.63
10C	1.033	1.019	1.021	90.45	96.92	87.01	9.04	9.69	8.70
10D	0.004	0.004	0.004	88.34	94.94	84.75	8.83	9.49	8.47
20A	0.000	0.000	0.000	180.69	194.31	173.59	9.03	9.71	8.68
					144.44[e]				
20B	0.278	0.266	0.282	182.26	195.62	175.19	9.11	9.78	8.76
20C	2.531	2.509	2.491	181.76	195.00	172.53	9.09	9.75	8.63
20D	8.156	8.132	8.003	182.01	195.38	174.67	9.10	9.77	8.73
				aug-cc-PVDZ					
6A	0.810	0.797	0.804	59.16	63.17	57.54	9.86	10.53	9.59
	0.809[g]			59.54[g]		58.06[h]	9.92[g]		
6B	0.000	0.000	0.000	60.48	64.47	58.82	10.08	10.75	9.80
	0.000[g]			60.98[g]		59.14[h]	10.16[g]		
6C	1.037	1.018	1.031	58.78	62.75	57.13	9.80	10.46	9.52
	1.037[g]			59.14[g]		57.68[h]	9.86[g]		
10A	0.996	0.981	0.990	98.75	105.26	96.18	9.88	10.53	9.62
						97.04[h]			
10B	0.876	0.860	0.868	98.97	105.61	96.32	9.90	10.56	9.63
10C	0.978	0.961	0.974	99.27	105.84	96.68	9.93	10.58	9.68

[a] All values are in atomic units. [b] B3LYP/TZ2P(f)++, ref. 8. [c] MP2/TZ2P++, ref. 7. [d] B3LYP/Sadlej's basis set, ref. 56. [e] TDHF/6-311++G(d,p) at static limit, ref. 56. [f] DFT/GGA, ref. 55. [g] B3LYP/aug-cc-pVTZ. [h] CCSD/aug-cc-pVDZ, ref. 49.

and receives two protons from the surrounding molecules, acting as both proton donor and acceptor.[81] The HB networks are different from the cases of water clusters. Obviously, many of the molecules in the clusters studied here are not saturated due to their small sizes. As the cluster size increases, the number of HB of each molecule increases until the coordination is saturated. One can expect that molecules with different coordination numbers and different hydrogen bonding will have different polarizabilities. According to these simple arguments, the heterogeneity of the molecular contributions to the cluster polarizability should decrease with the cluster size. The monotonous increase of the cluster polarizability with the cluster size may hide this heterogeneity.

The molecular polarizabilities, α_{mol}, derived from eqn (6), of W_6, W_{10} and W_{20} isomers are listed in Table 3. The values of α_{mol} computed at B3LYP and MP2 levels of theory are very close to each other, as is in the case for the global cluster polarizabilities, while PW91 gives relatively larger values than B3LYP and MP2 for the corresponding isomers. Fig. 2 illustrates the α_{mol} values obtained with B3LYP for ease of comparison. One should note that different color scales are applied to the clusters, depending on the minimum (light red) and maximum (black) values predicted for each cluster. From light to deep, α_{mol} becomes larger.

The magnitudes of α_{mol} are related to the locations of molecules in the cluster. The peripheral molecules on the surface tend to have larger values than those in a group. The two molecules on the left and right sides of 6A, 10C and 10D, and the two on the right side of 10B have relatively large values within the clusters. In 20A and 20C the largest values are found for the molecules at both ends. The molecules on the outer layer in 20B have larger values than the inner ones. However, this tendency is ambiguous for 6B, 6C, 10A and 20D in which all molecules can be viewed as "peripheral".

The magnitudes of the polarizability of a molecule within the cluster, α_{mol}, are found related to the HBs it forms with the other molecules. For ease of reference, we distinguish the molecules by different types of HB they form; named DA, DDA ,…, DDAA etc. For example, DA means the molecule donates one of its protons and accepts one proton from other molecule, while DDAA means the molecule forms the saturated structure with two protons donated and two protons accepted. This kind of classification has been commonly used in distinguishing the different bondings in water clusters, and some correlations of bond strength, dangling frequency and reactivity with HBs types have been established in previous studies.[82–87]
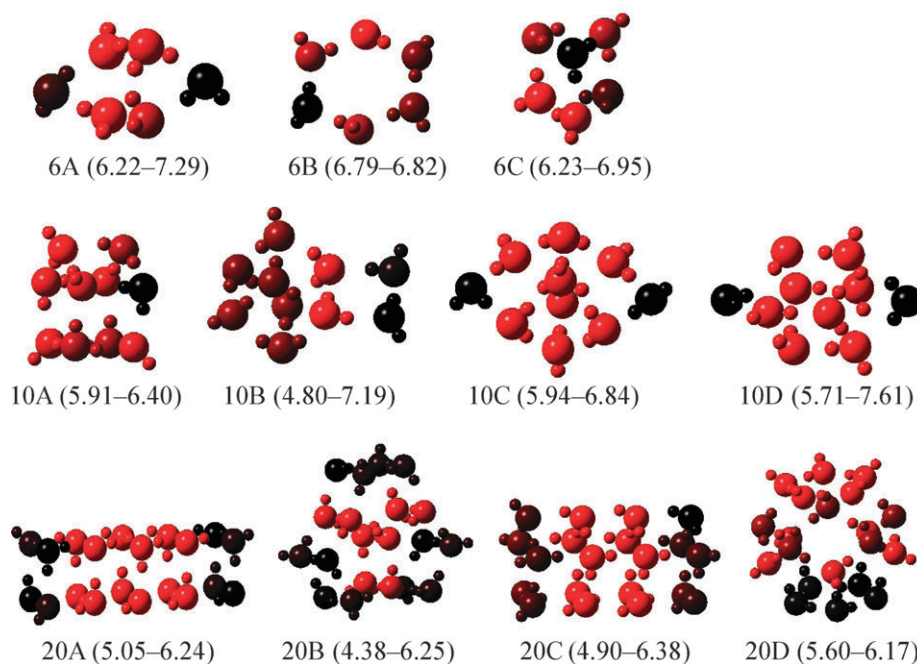
Fig. 2 Molecular polarizabilities in W_6, W_{10} and W_{20} isomers computed with B3LYP/aug-cc-pVDZ. The magnitude is scaled with colors from light red to black. In parentheses are the scales applied.

Table 3 Molecular polarizabilities (au) of W_6, W_{10} and W_{20} isomers[a]

	HB type[b]	N_{mol}[c]	B3LYP[d]	PW91[d]	MP2[d]
6A	DA	2	7.17 (7.05–7.29)	7.51 (7.37–7.65)	7.14 (7.02–7.25)
	DDA	2	6.46 (6.36–6.56)	6.47 (6.37–6.56)	6.77 (6.66–6.87)
	DAA	2	6.26 (6.22–6.30)	6.27 (6.23–6.32)	6.52 (6.48–6.55)
6B	DA	6	6.81 (6.79–6.82)	6.81 (6.78–6.83)	7.11 (7.08–7.14)
6C	DDA	3	6.75 (6.56–6.95)	7.08 (6.89–7.29)	6.73 (6.54–6.92)
	DAA	3	6.36 (6.23–6.51)	6.63 (6.50–6.78)	6.37 (6.24–6.51)
10A	DDA	5	5.98 (5.91–6.01)	6.21 (6.13–6.23)	6.01 (5.94–6.05)
	DAA	5	6.15 (6.00–6.40)	6.42 (6.25–6.69)	6.18 (6.04–6.42)
10B	DA	2	7.09 (6.99–7.19)	7.41 (7.29–7.52)	7.07 (6.98–7.16)
	DDA	3	6.23 (6.19–6.26)	6.50 (6.45–6.54)	6.25 (6.21–6.28)
	DAA	3	6.09 (6.06–6.10)	6.34 (6.31–6.35)	6.11 (6.09–6.12)
	DDAA	2	4.95 (4.80–5.09)	5.07 (4.89–5.24)	5.06 (4.92–5.19)
10C	DA	2	6.84 (6.83–6.84)	7.15 (7.14–7.15)	6.82 (6.81–6.82)
	DDA	4	6.01 (6.00–6.01)	6.24 (6.23–6.25)	6.05 (6.04–6.05)
	DAA	4	5.98 (5.94–6.03)	6.21 (6.17–6.26)	6.01 (5.97–6.06)
10D	DD	2	7.60 (7.60–7.61)	7.98 (7.97–7.98)	7.54 (7.53–7.54)
	DDA	4	5.82 (5.81–5.82)	6.04 (6.03–6.04)	5.86 (5.86–5.87)
	DAAA	4	5.72 (5.71–5.72)	5.90 (5.89–5.91)	5.76 (5.75–5.77)
20A	DDA	4	6.23 (6.22–6.24)	6.49 (6.48–6.50)	6.25 (6.24–6.26)
	DAA	4	6.08 (6.07–6.09)	6.32 (6.31–6.33)	6.11 (6.10–6.11)
	DDAA	12	5.07 (5.05–5.10)	5.20 (5.17–5.24)	5.17 (5.15–5.20)
20B	DDA	6	6.16 (6.03–6.25)	6.41 (6.27–6.50)	6.22 (6.14–6.30)
	DAA	6	6.02 (5.97–6.08)	6.23 (6.17–6.30)	6.07 (6.00–6.28)
	DDAA	8	4.68 (4.38–4.91)	4.78 (4.45–5.04)	4.79 (4.53–4.99)
20C	DDA	5	6.09 (5.90–6.38)	6.33 (6.12–6.65)	6.15 (6.06–6.39)
	DAA	5	5.97 (5.87–6.01)	6.19 (6.08–6.24)	5.98 (5.88–6.03)
	DDAA	10	4.98 (4.90–5.07)	5.10 (5.01–5.19)	5.08 (5.01–5.16)
20D	DDA	10	6.03 (5.90–6.17)	6.26 (6.10–6.43)	6.07 (5.96–6.19)
	DAA	10	5.65 (5.60–5.72)	5.83 (5.76–5.92)	5.70 (5.66–5.75)

[a] Calculations with aug-cc-pVDZ basis set. [b] See text for definition. [c] Number of molecules of the corresponding type. [d] Average molecular polarizabilities. In parentheses are the amplitudes.

There are three kinds of molecules in 6A. The two DA molecules have largest α_{mol}, followed by the two DDA molecules. The remaining two DAA molecules have the smallest α_{mol}. All the six DA molecules in 6B are almost

equivalent, and therefore they have nearly equivalent α_{mol}. The molecules in 6C are classified into two groups, DDA and DAA. The former includes three molecules with larger α_{mol} than the other three.

Half of the molecules in 10A are of DDA and the others of DAA. The DDA molecules tend to have larger α_{mol} than the DAA ones. The HBs in 10B are complicated and can be classified into four groups. The first involves two DA molecules with much larger α_{mol} than the other molecules in the cluster. The three DDA molecules in the second group and the three DAA molecules in the third group have intermediate α_{mol}. The last group contains two DDAA molecules. Each forms four HBs with other molecules. These two molecules have very small α_{mol}. In 10C, the two DA molecules have much larger α_{mol} than the other eight molecules, which have similar α_{mol}. Besides the four DDA molecules which have α_{mol} around 5.81 au at B3LYP level, the other six molecules in 10D have special bonding panels. Two of them donate their protons without receiving protons from other molecules. These two DD molecules have α_{mol} of 7.60 au, much larger than other molecules of W_{10} clusters. The remaining four molecules are in DAAA form and possess similar α_{mol} with the other DDA molecules in 10D.

There are three kinds of molecules in the W_{20} isomers, DAA, DDA and DDAA. 20A has four DAA molecules with slightly smaller α_{mol} than the four DDA ones. All the other twelve DDAA molecules have the smallest α_{mol}. 20B has six DAA, six DDA and eight DDAA molecules and those for 20C are five, five and ten, respectively. The same α_{mol} order for these three types is found for 20A, 20B and 20C. Only DAA and DDA molecules are found in 20D. Each type contains ten molecules and the DAA molecules have slightly smaller α_{mol} than DDA ones.

Clearly, α_{mol} is directly related to of the hydrogen bonding type. Molecules with more HBs tend to have smaller α_{mol} in a cluster. As a result, the surface molecules which usually form less HBs have larger α_{mol} than the molecules in the body. Apart from the number of HBs, the nature of HB also affects the magnitude of α_{mol}. DDA molecules tend to have larger α_{mol} than DAA ones. One may note that the molecules having the same type of hydrogen bonding may have slightly different polarizabilities in different clusters. For example, the DDA molecules have averaged α_{mol} varying from 5.81 au in 10D to 6.95 au in 6C. In addition, from W_6 to W_{20}, the averaged α_{mol} tends to decrease except for 20D which has a larger averaged α_{mol} than for 10A and the other three W_{20} isomers. One can also see the decreasing tendency in the upper and lower bounds of α_{mol} from W_6 to W_{20}.

Besides the number and type of HBs, the surrounding molecules can also affect the magnitude of α_{mol}. Take the two molecules on the left and right sides in 6A (see Fig. 2) as an example. Both molecules form two DA-type HBs with two molecules in the middle of the cluster, respectively. But their α_{mol}, 7.29 (right) and 7.05 au (left) computed at B3LYP level, are different. Further analysis shows that the four molecules in the middle are different. This can be seen from the net charge of these molecules, $-0.041e$ and $-0.047e$ for the pair of molecules bonding to the molecule on the right side of the cluster and $+0.040e$ and $+0.039e$ for the pair of molecules

bonding to the molecule on the left. The molecular charges were evaluated with the Hirshfeld scheme[62,63] at the B3LYP level. The same situation is found in 6C and 10A. The upper/left layer is different in construction from the lower/right layer, making the molecules with same HB number and type different in their α_{mol}.

3.4 Intra- and intermolecular polarizability

It should be mentioned that the molecular dipole moment induced by an electric field, used in the finite-field approach to compute the polarizability, can be defined in different ways. For example, the local dipole can be computed by choosing the local center of coordinates as the center of mass of the molecule instead of the geometric center, as it has been used by in het Panhuis et al.[61] in comparing the molecular polarizabilities in the water dimer. The difference in the definition of the dipole of a molecule in a cluster can lead to some variations in the magnitude of the molecular polarizabilities, but it does not change our findings. In fact, in het Panhuis et al.[61] reported that each molecule in the dimer has smaller polarizability than the isolated one, as we did.

The molecular polarizability presented above (computed with eqn (6)) is an intrinsic quantity transferable in comparing it with other molecules in the cluster, but it does not take the intermolecular terms (possible charge redistribution between molecules) into account. Inter-molecular contribution to the local polarizability of a molecule in the cluster is also important to understand the interaction between water molecules.

The cluster polarizability is built from intra- and inter-molecular parts and is not a simple summation of the molecular polarizabilities as defined by eqn (6). To study the contribution of the intra- and inter-molecular contributions to the cluster polarizability, one can use eqn (2) and rewrite the cluster polarizability as[88]

$$\langle \alpha^{\text{cluster}} \rangle = \sum_L \langle \alpha_L^P \rangle + \sum_L \langle \alpha_L^Q \rangle \qquad (7)$$

where

$$\langle \alpha_L^P \rangle = \frac{1}{3} \sum_\zeta \left(\frac{\partial \mu_{L,\zeta}^{\text{c}}}{\partial F_{\text{ext},\zeta}} \right)_{F=0} \qquad (8)$$

and

$$\langle \alpha_L^Q \rangle = \frac{1}{3} \sum_\zeta R_\zeta \left(\frac{\partial Q_{L,\zeta}}{\partial F_{\text{ext},\zeta}} \right)_{F=0}. \qquad (9)$$

The polarizability of the Lth molecule within the cluster is the sum of two terms: α_L^P, and α_L^Q. The quantity α_L^P is the intra-molecular polarizability which is independent on the choice of the origin of the coordinates and measures the polarization within the molecular basin against the external field. Its definition is to some extent different from the molecular polarizability α_{mol} defined with eqn (6). In comparison with α_{mol} which measures the molecular response to the superposition of the local induced field and external field, α_L^P describes the molecular response with respect to the external field alone. The sum of the polarizabilities α_L^P in eqn (7) can be defined as the total intra-molecular contribution to the cluster polarizability. The quantity α_L^Q depends on the choice of the

origin of the coordinates for charged molecules but their summation, the second term on the rhs in eqn (7), is origin-independent for a neutral cluster and can be rewritten as

$$\sum_L \langle \alpha_L^Q \rangle = \sum_i \langle \alpha_i^{HB} \rangle \qquad (10)$$

where i runs over all HBs and

$$\langle \alpha_i^{HB} \rangle = \frac{1}{3} \sum_\zeta (R_\zeta^A - R_\zeta^D) \left(\frac{\partial q_{i,\zeta}}{\partial F_{ext,\zeta}} \right)_{F=0}. \qquad (11)$$

q is the net charge flowing through the HB when an external field is applied. R is the Cartesian coordinate of the geometric center of the molecule involved in the HB formation where D and A denote hydrogen donor and acceptor respectively. Clearly, each term on the rhs in eqn (11) involves a pair of molecules that form a HB and measures the inter-molecular polarizability resulting from charge flow through the HBs. Different from eqn (6) where an intrinsic molecular polarizability is defined, eqn (7)–(11) decompose the cluster polarizability into intra- and inter-molecular parts and provide us with one way to inspect the contributions from each part.

Table 4 compares the intra- and inter-molecular parts of the polarizabilities of the water isomers. The results obtained with B3LYP and MP2 are similar for both parts. The values are slightly smaller than the corresponding PW91 results. But all these three methods give similar intra/total or inter/total ratios. From W_6, W_{10} to W_{20}, the contribution from $\langle \alpha^P \rangle$ tends to decrease while that from $\langle \alpha^Q \rangle$ tends to increase, though some exceptions are noted. With increasing cluster size, more molecules are located in the body. Shielded by the surface molecules, their response to the applied field are smaller than the response of the molecules on the surface, leading to smaller contributions to the intra-molecular polarizabilities. On the other hand, the increasing HB number in larger clusters favors the inter-molecular charge flow and leads to larger contributions to the inter-molecular polarizabilities.

We have seen that the water isomers at the same size have similar cluster polarizabilities, which may, however, have different origins. For example, the intra-(inter-)molecular polarizability of 10A is smaller (larger) than the other three isomers by 2.69 to 4.13 (2.99 to 4.01) au, while the deviation of cluster polarizability of 10A is less than 1.32 au. 20D has the largest intra-molecular polarizability, but it has the smallest inter-molecular counterpart and consequently it has cluster polarizability similar to the other W_{20} isomers. The ordering of the different polarizabilities, the intra-molecular part [eqn (8)], the inter-molecular part [eqn (9)], and their sum [eqn (7)] are different. For example, the ordering of the intra-molecular cluster polarizabilities for the W_6 and W_{20} isomers are 6C > 6B > 6A, 10C > 10B > 10D > 10A and 20D > 20C > 20B > 20A, whereas the ordering of the inter-molecular cluster polarizabilities of these clusters are 6B > 6A > 6C, 10A > 10B > 10C > 10D and 20B > 20A > 20C > 20D.

Eqn (10) and (11) reveal the direct correlation of the intermolecular polarizability with the HB formation in the clusters. Strong and/or more HBs favor charge transfer and lead to larger intermolecular polarizabilities. 6B has fewer but stronger HBs than 6C, as illustrated by the numbers and bond lengths of HB in Table 1. The charge flow in 6C is favored by the large number of HBs, but is hindered by the weakness of the HBs, causing 6B to have larger inter-molecular polarizability than 6C. Another situation is found in 20D for which the number of HBs dominates the inter-molecular polarizability. 20D has six less HBs than 20A and has the smallest inter-molecular polarizability, though the averaged HB bond length in 20D is the shortest among the isomers. Thus one has to consider both the number and strength of HBs in estimating the inter-molecular polarizabilities, especially for the clusters of small size.

4. Summary

Polarizabilities of water clusters have been computed for different isomers of $(H_2O)_N$ clusters for $N = 6$, 10 and 20. The global cluster polarizability was found to depend mainly on the number of molecules in the cluster rather than its geometry; the values of the cluster polarizability for different isomers are very similar to each other. We analyzed the different molecular contributions to the global cluster polarizability by applying different partitioning schemes, all based on the Hirshfeld method.

By partitioning the total electron density into molecular contributions using the Hirshfeld scheme, we defined and computed the intrinsic polarizabilities of individual molecules within a cluster [eqn (6)]. The cluster polarizability does not show a clear trend with respect to the stability or the number of HBs in the isomers. In contrast, we found a correlation between the value of the intrinsic molecular polarizability and the type and number of HBs a molecule forms within the cluster. In a cluster, the molecules with more HBs tend to have smaller intrinsic polarizabilities and consequently the molecules situated inside the cluster usually have smaller polarizabilities than those on the surface.

The cluster polarizability can be further decomposed into intra- and intermolecular parts by using eqn (7)–(9). The intra-molecular contribution describes the contribution of the polarization confined within a molecule basin whereas the inter-molecular contribution includes charge reorganization (charge transfer) between molecules. The latter is interpreted as the inter-molecular polarization through the HBs. Both

Table 4 Intra- and intermolecular polarizabilities in the W_6, W_{10} and W_{20} isomers calculated with aug-cc-pVDZ basis set

	B3LYP			PW91			MP2		
	α^P	$\bar{\alpha}^Q$	α^P/α^{tot}	$\bar{\alpha}^P$	$\bar{\alpha}^Q$	α^P/α^{tot}	$\bar{\alpha}^P$	$\bar{\alpha}^Q$	α^P/α^{tot}
6A	37.33	21.83	0.63	38.85	24.32	0.62	37.48	20.06	0.65
6B	37.70	22.78	0.62	39.16	25.31	0.61	37.94	20.89	0.64
6C	38.25	20.53	0.65	39.90	22.86	0.64	38.29	18.84	0.67
10A	57.60	41.15	0.58	59.79	45.47	0.57	58.11	38.07	0.60
10B	60.82	38.16	0.61	63.21	42.41	0.60	61.07	35.26	0.63
10C	61.73	37.54	0.62	64.23	41.62	0.61	61.94	34.74	0.64
10D	60.29	37.14	0.62	62.49	41.54	0.60	60.64	34.16	0.64
20A	110.32	86.50	0.56	114.04	96.24	0.54	119.19	73.99	0.62
20B	110.94	87.06	0.56	114.54	96.86	0.54	117.81	75.41	0.61
20C	111.78	85.02	0.57	115.66	94.32	0.55	116.76	73.78	0.61
20D	118.27	81.37	0.59	122.58	90.56	0.58	122.49	71.54	0.63

parts are related to the cluster size and the HBs formed in the cluster.

In conclusion, the present study reveals that the polarizabilities of water isomers are close in magnitude, confirming that the polarizability of a water cluster mainly depends on its size. But this simple result hides the heterogeneity that the polarization of water clusters still depends on their structures. By means of decomposing cluster polarizability into molecular contributions, we revealed the structure dependence and the origin of the linear dependence of cluster polarizability with size.

Acknowledgements

References

1 M. M. Teeter, *Proc. Natl. Acad. Sci. U. S. A.*, 1984, **81**, 6014–6018.
2 S. S. Xantheas and T. H. Dunning Jr, *J. Chem. Phys.*, 1993, **99**, 8774–8792.
3 K. Laasonen, M. Parrinello, R. Car, C. Lee and D. Vanderbilt, *Chem. Phys. Lett.*, 1993, **207**, 208–213.
4 K. Liu, J. D. Cruzan and R. J. Saykally, *Science*, 1996, **271**, 929–933.
5 J. K. Gregory and D. C. Clary, *J. Phys. Chem.*, 1996, **100**, 18014–18022.
6 J. K. Gregory, D. C. Clary, K. Liu, M. G. Brown and R. J. Saykally, *Science*, 1997, **275**, 814–817.
7 J. M. Pedulla, K. Kim and K. D. Jordan, *Chem. Phys. Lett.*, 1998, **291**, 78–84.
8 J. Kim and K. S. Kim, *J. Chem. Phys.*, 1998, **109**, 5886–5895.
9 D. J. Wales and M. P. Hodges, *Chem. Phys. Lett.*, 1998, **286**, 65–72.
10 J. M. Ugalde, I. Alkorta and J. Elguero, *Angew. Chem., Int. Ed.*, 2000, **39**, 717–721.
11 S. S. Xantheas, *Chem. Phys.*, 2000, **258**, 225–231.
12 K. S. Kim, P. Tarakeshwar and J. Y. Lee, *Chem. Rev.*, 2000, **100**, 4145–4185.
13 K. Müller-Dethlefs and P. Hobza, *Chem. Rev.*, 2000, **100**, 143–167.
14 U. Buck and F. Huisken, *Chem. Rev.*, 2000, **100**, 3863–3890.
15 R. Ludwig, *Angew. Chem., Int. Ed.*, 2001, **40**, 1808–1827.
16 F. N. Keutsch and R. J. Saykally, *Proc. Natl. Acad. Sci. U. S. A.*, 2001, **98**, 10533–10540.
17 S. Maheshwary, N. Patel, N. Sathyamurthy, A. D. Kulkarni and S. R. Gadre, *J. Phys. Chem. A*, 2001, **105**, 10525–10537.
18 D. B. Chesnut, *J. Phys. Chem. A*, 2002, **106**, 6876–6879.
19 J. K. Kazimirski and V. Buch, *J. Phys. Chem. A*, 2003, **107**, 9762–9775.
20 J. T. Su, X. Xu and W. A. Goddard, *J. Phys. Chem. A*, 2004, **108**, 10518–10526.
21 R. Wieczorek, L. Haskamp and J. J. Dannenberg, *J. Phys. Chem. A*, 2004, **108**, 6713–6723.
22 V. Buch, S. Bauerecker, J. P. Devlin, U. Buck and J. K. Kazimirski, *Int. Rev. Phys. Chem.*, 2004, **23**, 375–433.
23 T. James, D. J. Wales and J. Hernández-Rojas, *Chem. Phys. Lett.*, 2005, **415**, 302–307.
24 G. Öhrwall, R. F. Fink, M. Tchaplyguine, L. Ojamäe, M. Lundwall, R. R. T. Marinho, A. N. de Brito, S. L. Sorensen, M. Gisselbrecht, R. Feifel, T. Rander, A. Lindblad, J. Schulz,

L. J. Saethre, N. Mårtensson, S. Svensson and O. Björneholm, *J. Chem. Phys.*, 2005, **123**, 54310.
25 S. Hirabayashi and K. M. T. Yamada, *J. Chem. Phys.*, 2005, **122**, 244501.
26 A. Lenz and L. Ojamäe, *Phys. Chem. Chem. Phys.*, 2005, **7**, 1905–1911.
27 M. E. Dunn, T. M. Evans, K. N. Kirschner and G. C. Shields, *J. Phys. Chem. A*, 2006, **110**, 303–309.
28 B. Santra, A. Michaelides and M. Scheffler, *J. Chem. Phys.*, 2007, **127**, 184104.
29 H. B. Yu and Q. Cui, *J. Chem. Phys.*, 2007, **127**, 234504.
30 Q. C. Nguyen, Y. S. Ong, H. Soh and J. L. Kuo, *J. Phys. Chem. A*, 2008, **112**, 6257–6261.
31 Y. Watanabe, S. Maeda and K. Ohno, *J. Chem. Phys.*, 2008, **129**, 074315.
32 B. Santra, A. Michaelides, M. Fuchs, A. Tkatchenko, C. Filippi and M. Scheffler, *J. Chem. Phys.*, 2008, **129**, 194111.
33 V. S. Bryantsev, M. S. Diallo, A. C. T. van Duin and W. A. Goddard III, *J. Chem. Theory Comput.*, 2009, **5**, 1016–1026.
34 S. Kazachenko and A. J. Thakkar, *Chem. Phys. Lett.*, 2009, **476**, 120–124.
35 J. S. Prell and E. R. Williams, *J. Am. Chem. Soc.*, 2009, **131**, 4110–4119.
36 M. Alfredsson, J. P. Brodholt, K. Hermanson and R. Vallauri, *Mol. Phys.*, 1998, **94**, 873–876.
37 E. R. Batista, S. S. Xantheas and H. Jónsson, *J. Chem. Phys.*, 1998, **109**, 4546–4551.
38 P. L. Silvestrelli and M. Parrinello, *Phys. Rev. Lett.*, 1999, **82**, 3308–3311.
39 Y. Tu and A. Laaksonen, *Chem. Phys. Lett.*, 2000, **329**, 283–288.
40 H. A. Stern, F. Rittner, B. J. Berne and R. A. Friesner, *J. Chem. Phys.*, 2001, **115**, 2237–2251.
41 H. Xu, H. A. Stern and B. J. Berne, *J. Phys. Chem. B*, 2002, **106**, 2054–2060.
42 K. Coutinho, R. C. Guedes, B. J. Costa Cabral and S. Canuto, *Chem. Phys. Lett.*, 2003, **369**, 345–353.
43 M. Yang, P. Senet and C. van Alsenoy, *Int. J. Quantum Chem.*, 2005, **101**, 535–542.
44 A. Krishtal, P. Senet, M. Yang and C. van Alsenoy, *J. Chem. Phys.*, 2006, **125**, 34312.
45 R. Moro, R. Rabinovitch, C. L. Xia and V. V. Kresin, *Phys. Rev. Lett.*, 2006, **97**, 123401.
46 D. Rai, A. D. Kulkarni, S. P. Gejji and R. K. Pathak, *J. Chem. Phys.*, 2008, **128**, 034310.
47 N. Deb and A. K. Mukherjee, *Chem. Phys. Lett.*, 2008, **462**, 243–245.
48 Á. Carrera, M. Mobbili and E. Marceca, *J. Phys. Chem. A*, 2009, **113**, 2711–2714.
49 J. R. Hammond, N. Govind, K. Kowalski, J. Autschbach and S. S. Xantheas, *J. Chem. Phys.*, 2009, **131**, 214103.
50 T. D. Poulsen, P. R. Ogilby and K. V. Mikkelsen, *J. Chem. Phys.*, 2002, **116**, 3730–3738.
51 L. X. Dang and T. M. Chang, *J. Chem. Phys.*, 1997, **106**, 8149–8159.
52 S. Chalmet and M. F. Ruiz-López, *J. Chem. Phys.*, 2001, **115**, 5220–5227.
53 K. S. Kim, B. J. Minh, U. S. Choi and K. Lee, *J. Chem. Phys.*, 1992, **97**, 6649–6662.
54 G. Maroulis, *J. Chem. Phys.*, 2000, **113**, 1813–1820.
55 P. Otto, F. L. Gu and J. Ladik, *J. Chem. Phys.*, 1999, **110**, 2717–2726.
56 L. Jensen, M. Swart, P. Th. van Duijnen and J. G. Snijders, *J. Chem. Phys.*, 2002, **117**, 3316–3320.
57 J. Rodriguez, D. Laria, E. J. Marceca and D. A. Estrin, *J. Chem. Phys.*, 1999, **110**, 9039–9047.
58 T. K. Ghanty and S. K. Ghosh, *J. Chem. Phys.*, 2003, **118**, 8547–8550.
59 A. Morita and S. Kato, *J. Chem. Phys.*, 1999, **110**, 11987–11998.
60 A. Morita, *J. Comput. Chem.*, 2002, **23**, 1466–1471.
61 M. in het Panhuis, P. L. A. Popelier, R. W. Munn and J. G. Angyan, *J. Chem. Phys.*, 2001, **114**, 7951–7961.
62 F. L. Hirshfeld, *Theor. Chim. Acta*, 1977, **44**, 129–138.
63 B. Rousseau, A. Peeters and C. van Alsenoy, *Chem. Phys. Lett.*, 2000, **324**, 189–194.

64 D. J. Wales, J. P. K. Doye, A. Dullweber, M. P. Hodges, F. Y. Naumkin, F. Calvo, J. Hernández-Rojas and T. F. Middleton, The Cambridge Cluster Database. URL http://www-wales.ch.cam.ac.uk/CCD.html.

65 D. P. Shelton and J. E. Rice, *Chem. Rev.*, 1994, **94**, 3–29.

66 L. Li, Z. Zhou, X. Wang, W. Huang, Y. He and M. Yang, *Phys. Chem. Chem. Phys.*, 2008, **10**, 6829–6835.

67 F. Sim, S. Chin, M. Dupuis and J. E. Rice, *J. Phys. Chem.*, 1993, **97**, 1158–1163.

68 A. D. Becke, *J. Chem. Phys.*, 1993, **98**, 5648–5652.

69 C. Lee, W. Yang and R. G. Parr, *Phys. Rev. B: Condens. Matter*, 1988, **37**, 785–789.

70 J. P. Perdew, K. Burke and Y. Wang, *Phys. Rev. B: Condens. Matter*, 1996, **54**, 16533–16539.

71 H. D. Cohen and C. C. J. Roothaan, *J. Chem. Phys.*, 1965, **43**, S34–S39.

72 H. A. Kurtz, J. J. P. Stewart and K. M. Dieter, *J. Comput. Chem.*, 1990, **11**, 82–87.

73 R. Kubo and T. Nagamya, *Solid State Physics*, Mc Graw-Hill, New York, 1969.

74 P. Senet, M. Yang, P. Delarue, S. Lagrange and C. van Alsenoy, in *Computational Methods in Sciences and Engineering*, ed. T. Simos and G. Maroulis, Brill Academic, Leiden, Netherlands, 2005, vol. 4, p. 234.

75 P. Senet, M. Yang and C. van Alsenoy, in *Atoms, Molecules and Clusters in Electric Fields: Theoretical Approaches to the Calculation of Electric Polarizabilities*, ed. G. Maroulis, Imperial College Press, London, United Kingdom, 2006.

76 *GAUSSIAN 03 (Revision C.02)*, Gaussian, Inc., Pittsburgh, PA, 2004.

77 C. van Alsenoy and A. Peeters, *J. Mol. Struct. (THEOCHEM)*, 1993, **286**, 19–34.

78 S. Kristián and P. Pulay, *Chem. Phys. Lett.*, 1994, **229**, 175–180.

79 E. Ruiz, D. R. Salahub and A. Vela, *J. Am. Chem. Soc.*, 1995, **117**, 1141–1142.

80 M. R. Pederson, T. Baruah, P. B. Allen and C. Schmidt, *J. Chem. Theory Comput.*, 2005, **1**, 590–596.

81 J. L. Kuo, M. L. Klein and W. F. Kuhs, *J. Chem. Phys.*, 2005, **123**, 134505.

82 J. Sadlej, *Chem. Phys. Lett.*, 2001, **333**, 485–492.

83 D. J. Anick, *J. Chem. Phys.*, 2005, **123**, 244309.

84 C. Steinbach and U. Buck, *J. Phys. Chem. A*, 2006, **110**, 3128–3131.

85 H. Cybulski and J. Sadlej, *Chem. Phys.*, 2006, **323**, 218–230.

86 N. Ji, V. Ostroverkhov, C. S. Tian and Y. R. Shen, *Phys. Rev. Lett.*, 2008, **100**, 96102.

87 C. S. Tian and Y. R. Shen, *Proc. Natl. Acad. Sci. U. S. A.*, 2009, **106**, 15148–15153.

88 K. A. Jackson, M. Yang and J. Jellinek, *J. Phys. Chem. C*, 2007, **111**, 17952–17960.